



Fundus Changes Evaluated by OCTA in Patients With Cerebral Small Vessel Disease and Their Correlations: A Cross-Sectional Study

OPEN ACCESS

Wang Fu^{1†}, Xiaoyu Zhou^{1†}, Minli Wang², Ping Li², Jingjing Hou³, Peng Gao^{2*} and Jue Wang^{4*}

Edited by:

John Jing-Wei Chen,
Mayo Clinic, United States

Reviewed by:

Laurel N. Vuong,
Tufts Medical Center, United States
Gregory Van Stavern,
Washington University in St. Louis,
United States

*Correspondence:

Jue Wang
wangjueshiyuan@163.com
Peng Gao
neocloudy@hotmail.com

[†]These authors have contributed
equally to this work and share first
authorship

Specialty section:

This article was submitted to
Neuro-Ophthalmology,
a section of the journal
Frontiers in Neurology

Received: 31 December 2021

Accepted: 14 March 2022

Published: 25 April 2022

Citation:

Fu W, Zhou X, Wang M, Li P, Hou J,
Gao P and Wang J (2022) Fundus
Changes Evaluated by OCTA in
Patients With Cerebral Small Vessel
Disease and Their Correlations: A
Cross-Sectional Study.
Front. Neurol. 13:843198.
doi: 10.3389/fneur.2022.843198

¹ Department of Neurology, Shanghai Tenth People's Hospital, Tongji University School of Medicine, Shanghai, China, ² Department of Ophthalmology, Shanghai Tenth People's Hospital, Tongji University School of Medicine, Shanghai, China, ³ Tongji University School of Medicine, Shanghai, China, ⁴ Educational Office, Shanghai Tenth People's Hospital, Tongji University School of Medicine, Shanghai, China

Objective: To detect fundus changes in patients with cerebral small vessel disease (CSVD) using optical coherence tomography angiography (OCTA) and to investigate the correlations between CSVD and fundus changes.

Methods: From January 2019 to January 2020, patients diagnosed with CSVD by magnetic resonance imaging (MRI) were enrolled in our study and received fundus examinations using OCTA. CSVD was defined as white matter hyperintensities, enlarged perivascular spaces, lacunes, or microbleeds on MRI. OCTA parameters included foveal avascular zone areas, retinal nerve fiber layer thickness, and capillary densities of the superficial retinal capillary plexuses, deep retinal capillary plexuses, and the radial peripapillary capillary network of the disc. Univariate and multivariate logistic regression analyses were performed to explore the correlation between CSVD and fundus changes.

Results: A total of 115 patients (40% male) were enrolled and analyzed, and the mean age was 65.11 ± 11.23 years. After multivariate logistic regression analysis, the radial peripapillary capillary network density was negatively correlated with severity of deep white matter lesions (OR: 0.909; 95% CI: 0.828–0.998; $p = 0.046$) and perivascular spaces (OR: 0.881; 95% CI: 0.779–0.995; $p = 0.041$). Parafoveal vessel densities of the superficial retinal capillary plexuses were independently correlated with lacunes (OR: 0.889; 95% CI: 0.817–0.967; $p = 0.006$).

Conclusion: OCTA parameters were correlated with CSVD, indicating that OCTA is a potential method for CSVD screening.

Keywords: retinal capillary density, white matter lesions, perivascular spaces, cerebral microbleeds, optical coherence tomography angiography

INTRODUCTION

Cerebral small vessel disease (CSVD) is commonly used to describe a disorder consisting of clinical, cognitive, neuroimaging, and neuropathological manifestations induced by the brain's small perforating arterioles, capillaries, and perhaps venules (1, 2). CSVD presents with lacunes, cerebral hemorrhage, white matter lesions (WMLs), microbleeds, and microstroke (3). The prevalence of CSVD in older adults (aged > 65 years) is estimated at 87%. Lacunar stroke, which is caused by small vessel disease, accounts for 25–50% of all ischemic strokes in China. Severe WMLs could lead to cognitive decline (vascular dementia), depression, abnormal gait, dyskinesia, dysphagia, and urinary incontinence (4). Hence, early screening for CSVD is of great importance.

The features of CSVD on magnetic resonance imaging (MRI) include *de novo* small subcortical infarcts, lacunes, white matter hyperintensities, enlarged perivascular spaces (PVS), microbleeds, and brain atrophy (5, 6). Currently, MRI is the most commonly used imaging modality in clinical practice to evaluate CSVD. However, the high cost and incompatibility of MRI with certain metallic components prevent its use as a screening method. Therefore, a simpler, more cost-effective screening modality is required. The retina and the optic nerve head are components of the central nervous system (7), and the anatomic, embryologic, and physiologic characteristics of the retinal blood vessels are similar to those of the cerebral small vessels (8–10). The retinal vasculature that is correlated with the development of the cerebral vasculature can be directly visualized with ophthalmoscopy or retinal photography findings and therefore could provide information regarding CSVD (9, 10).

Optical coherence tomography angiography (OCTA) is a novel technique used to optically dissect and visualize the retinal microvascular system through a layer-by-layer analysis. OCTA provides high-resolution images and does not require injection of contrast medium (8, 11, 12) and is thereby a promising potential method to detect CSVD. Previous studies involving OCTA and CSVD have either focused on patients with Alzheimer's disease (AD) or patients with mild cognitive impairment, or were limited to small cohorts (8). Moreover, previous studies have only explored the correlation between WMLs and fundus changes. However, different mechanisms of WMLs have not been discussed in terms of location. Therefore, this comprehensive study included an appropriate sample size to explore the correlation between different CSVD type and fundus changes indicated by OCTA parameters, suggesting the feasibility and effectiveness of OCTA in CSVD screening.

MATERIALS AND METHODS

Participants

From January 2019 to January 2020, patients diagnosed with CSVD on MRI were enrolled. These participants underwent ophthalmic examinations, including slit-lamp, intraocular pressure, fundus photography, and OCTA at Shanghai Tenth People's Hospital, Tongji University. This study was approved by the Ethics Committee of Shanghai Tenth People's Hospital

(approval number: 21k253) and complied with the Declaration of Helsinki guidelines. Informed consent was obtained from all participants. Inclusion criteria were as follows: (1) aged \geq 18 years, (2) underwent brain MRI and OCTA examinations as well as other ophthalmic examinations, (3) have at least one imaging feature of CSVD confirmed by MRI. Exclusion criteria were as follows: (1) history of ocular surgery or primary eye diseases involving the retina or refractive media opacity that hindered observations of the fundus, such as retinal choroid inflammatory diseases, cataracts, glaucoma, posterior vitreous detachment, epiretinal membrane, macular degeneration, optic neuropathies, or severe diabetic or hypertensive retinopathy, (2) contraindications to MRI, (3) unable to undergo OCTA as well as other ophthalmic examinations, (4) AD, (5) diseases such as large-area cerebral infarction, intracerebral hemorrhage, or brain tumor affecting the evaluation of CSVD.

One eye from each enrolled participant was randomly selected. All eligible patients and their medical records were reviewed for demographic, diagnosis, MRI, and follow-up information. Demographic data included age, sex, history of hypertension, diabetes mellitus, and hyperlipidemia. The MRI examination included T1, T2 weighted imaging (T1WI, T2WI), fluid-attenuated inversion recovery (FLAIR) sequence, and T2*-weighted gradient-echo. The MRI's were reviewed by a neuroradiologist who was masked to the OCTA findings.

White Matter Lesions

WMLs were lesions that exhibited hyperintensity on FLAIR and T2WI without obvious hypointensity on T1WI. Periventricular WMLs (PWMLs) were defined if the lesions were adjacent to the ventricle, otherwise, defined as deep WMLs (DWMLs) (13). An experienced neuro-radiologist assessed the Fazekas scores of WMLs using FLAIR. The specific Fazekas scoring was as follows: periventricular hyperintensity was graded as 0 = absence, 1 = "caps" or pencil-thin lining, 2 = smooth "halo," 3 = irregular periventricular hyperintensity extending into the deep white matter. Deep white matter hyperintense signals were defined as 0 = absent, 1 = punctate foci, 2 = beginning confluence of foci, 3 = large confluent areas (13). WMLs were divided into a mild group (0–1 points) and a moderate to severe group (2–3 points) in this study.

Lacunes

Lacunes were identified as subcortical cavities with fluid between 3 and 15 mm in diameter, located in the territories of perforating arterioles, consistent with a previous acute small deep brain infarct or hemorrhage in the territory of one perforating arteriole (14). They appeared hypointense on T1 and hyperintense on T2, and as a hypointense cavity in the FLAIR sequence, surrounded by a hyperintense halo for reactive gliosis, which was different from PVS (14). In this study, lacunes were dichotomized as presence and absence.

Perivascular Spaces

PVS were considered as small and well-defined images (<3 mm in diameter) with a signal intensity equal to that of the cerebrospinal fluid located in the basal ganglia, semioval center,

TABLE 1 | Univariate analysis of clinical features for patients with CSVD.

| | DWMLs | | PWMLs | | PVS | | Lacunes | | CMB | |
|----------------|----------------------|----------------------|----------------------|----------------------|--------------------|--------------------|------------------|------------------|------------------|------------------|
| | Fazekas 0-1 (n = 62) | Fazekas 2-3 (n = 53) | Fazekas 0-1 (n = 62) | Fazekas 2-3 (n = 53) | 1-2 score (n = 71) | 3-4 score (n = 44) | Yes (n = 65) | No (n = 50) | Yes (n = 75) | No (n = 40) |
| | No. (%) | No. (%) | No. (%) | No. (%) | No. (%) | No. (%) | No. (%) | No. (%) | No. (%) | No. (%) |
| Male | 25 (40.3) | 21 (39.6) | 27 (43.5) | 19 (35.8) | 25 (35.2) | 21 (47.7) | 19 (38.0) | 27 (41.5) | 14 (35.0) | 32 (42.7) |
| Hypertension | 30 (48.4) | 38 (71.7) | 28 (45.2) | 40 (75.5) | 34 (47.9) | 32 (72.7) | 22 (44.0) | 46 (70.8) | 18 (45.0) | 50 (66.7) |
| DM | 20 (32.3) | 13 (24.5) | 22 (35.5) | 11 (20.8) | 24 (33.8) | 9 (20.5) | 13 (26.0) | 20 (30.8) | 7 (17.5) | 26 (34.7) |
| Hyperlipidemia | 29 (53.2) | 18 (66.0) | 31 (50.0) | 16 (30.2) | 33 (46.5) | 14 (31.8) | 17 (34.0) | 30 (46.2) | 11 (27.5) | 36 (48.0) |
| | $\bar{x} \pm SD$ | $\bar{x} \pm SD$ | $\bar{x} \pm SD$ | $\bar{x} \pm SD$ | $\bar{x} \pm SD$ | $\bar{x} \pm SD$ | $\bar{x} \pm SD$ | $\bar{x} \pm SD$ | $\bar{x} \pm SD$ | $\bar{x} \pm SD$ |
| Age (years) | 61.4 ± 11.2 | 69.5 ± 9.6 | 61.6 ± 11.3 | 69.2 ± 9.8 | 62.1 ± 10.0 | 70.0 ± 11.6 | 66.3 ± 10.6 | 64.2 ± 11.7 | 68.1 ± 8.2 | 63.5 ± 12.3 |
| | | | | | <0.001 | | <0.001 | | 0.323 | |
| | | | | | 0.939 | | 0.401 | | 0.183 | |
| | | | | | 0.014 | | <0.001 | | 0.004 | |
| | | | | | 0.361 | | 0.082 | | 0.575 | |
| | | | | | 0.164 | | 0.031 | | 0.189 | |

CSVD, cerebral small vessel disease; DWMLs, deep white matter lesions; PWMLs, periventricular white matter lesions; PVS, perivascular spaces; CMB, cerebral microbleed; DM, diabetes mellitus; SD, standard deviation.

or radiated corona, that followed the course of penetrating vessels; they appeared linear when imaged parallel to the course of the vessel and round or ovoid when imaged perpendicular to the course of the vessel (14). An increase in signal intensity on MRI was equal to cerebrospinal fluid on T2WI images, and hypointensity on T1WI and FLAIR.

The most commonly used score was based on the PVS number, defined by Potter and Doubal: 0 (none), 1(1-10), 2(11-20), 3(21-40), and 4 (>40) (15). In this study, PVS were classified as mild (1–2 points) and moderate to severe (3–4 points).

Microbleeds

Cerebral microbleeds (CMB) primarily correspond pathologically to hemosiderin-laden macrophages close to arterioles affected by small vessel diseases (16). These microbleeds could be clearly identified on T2*-weighted gradient-recalled echo or susceptibility-weighted imaging sequences, appearing as small hypointense lesions which were generally invisible on CT, FLAIR, T1WI, or T2WI MR sequences. We assessed cerebral microbleeds using T2*-weighted gradient-recalled echo in our study. In this study, CMB were dichotomized as presence and absence.

Optical Coherence Tomography Angiography

The RTVue XR Avanti spectral-domain OCT system (Optovue, Inc., Fremont, CA, USA) was used to evaluate the retinal microvasculature, and measurements were obtained using the manufacturer's AngioVue software. Areas in the fovea (6 mm × 6 mm) and around the optic disc (4.5 mm × 4.5 mm) were scanned. Images with poor quality or inadequate signal [signal strength index (SSI) < 50] or an OCTA motion artifact score of three or four were excluded.

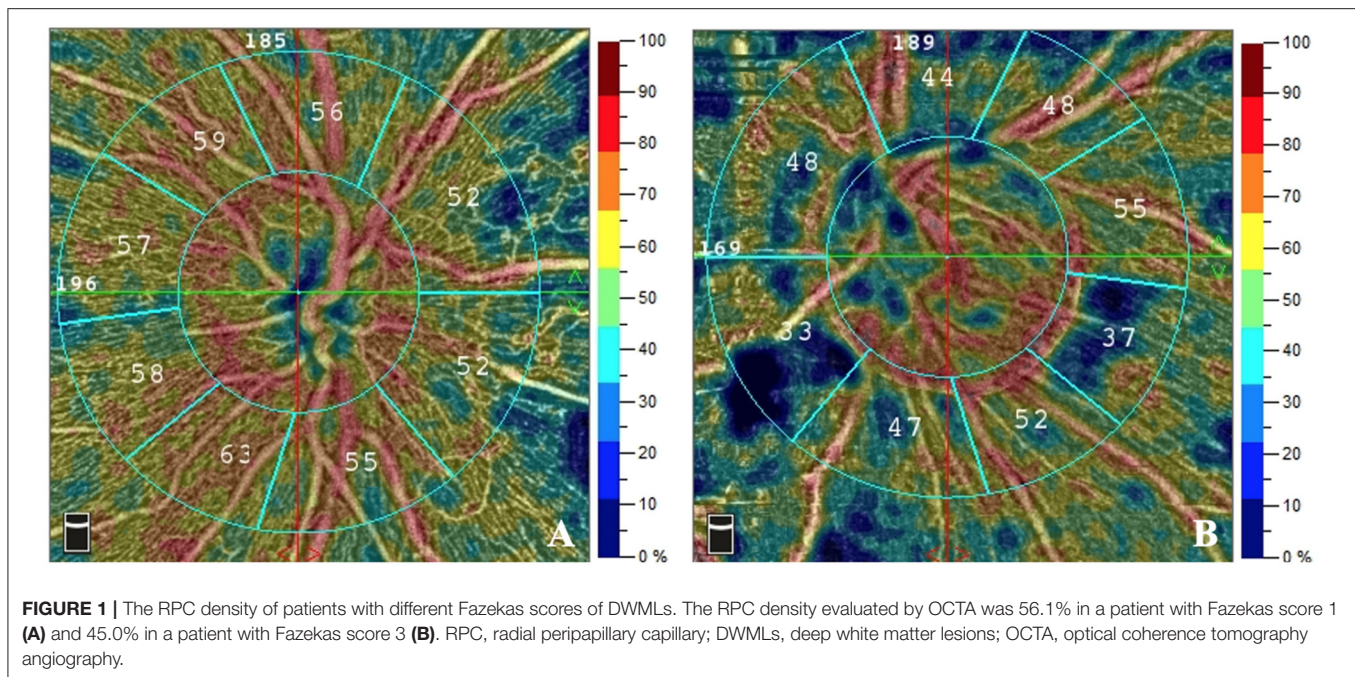
The OCTA software was used to record and analyze the enface images of the foveal avascular zone (FAZ), superficial retinal capillary plexuses (SRCP, located between the internal limiting membrane and 10 μm above the inner plexiform layer), and deep retinal capillary plexuses (DRCP, located between 10 μm above the inner plexiform layer and 10 μm below the outer plexiform layers) networks. The macular microvasculature and retinal nerve fiber layer (RNFL) thickness in both the SRCP and DRCP were evaluated. Three concentric circles of macular microvasculature density were analyzed as described in a previous study (17), which included a central circular subfield (disc radius: 0.3 mm), an internal annular zone (0.3–1.5 mm from the fovea; defined as “parafoveal area”) and an external annular zone (1.5–3.0 mm from the fovea, defined as the “perifoveal area”).

The radial peripapillary capillary (RPC) networks, which extended from the internal limiting membrane to the nerve fiber layer, were automatically separated by the instrument software. The RPC density, inside disc microvasculature density, and RNFL thickness were automatically assessed by the OCTA and OCT software.

TABLE 2 | Univariate analysis of OCT and OCTA parameters for patients with CSVD.

| | DWMLs | | p | PWMLs | | p | PVS | | p | Lacunes | | p | CMB | | p |
|-----------------------------------|-------------------------|-------------------------|------------------|-------------------------|-------------------------|------------------|--------------------|--------------------|------------------|------------------|-------------|--------|--------------|--------------|-------|
| | Fazekas 0–1 (n = 62) | Fazekas 2–3 (n = 53) | | Fazekas 0–1 (n = 62) | Fazekas 2–3 (n = 53) | | 1–2 score (n = 71) | 3–4 score (n = 44) | | Yes (n = 65) | No (n = 50) | | Yes (n = 75) | No (n = 40) | |
| | $\bar{x} \pm SD$ | $\bar{x} \pm SD$ | $\bar{x} \pm SD$ | $\bar{x} \pm SD$ | $\bar{x} \pm SD$ | $\bar{x} \pm SD$ | $\bar{x} \pm SD$ | $\bar{x} \pm SD$ | $\bar{x} \pm SD$ | $\bar{x} \pm SD$ | | | | | |
| SRCP | | | | | | | | | | | | | | | |
| Parafoveal capillary density (%) | 44.8 ± 6.4 | 43.8 ± 7.5 | 0.438 | 44.5 ± 6.5 | 44.2 ± 7.5 | 0.804 | 44.7 ± 6.4 | 43.9 ± 7.7 | 0.545 | 41.4 ± 7.0 | 46.7 ± 6.0 | <0.001 | 44.7 ± 8.0 | 44.2 ± 6.3 | 0.678 |
| Perifoveal capillary density (%) | 45.4 ± 4.4 | 45.2 ± 4.9 | 0.827 | 45.6 ± 4.5 | 44.9 ± 4.8 | 0.431 | 45.4 ± 4.5 | 45.1 ± 4.9 | 0.720 | 44.1 ± 4.6 | 46.2 ± 4.4 | 0.015 | 45.6 ± 4.7 | 45.1 ± 4.6 | 0.637 |
| DRCP | | | | | | | | | | | | | | | |
| Parafoveal capillary density (%) | 48.6 ± 7.3 | 48.2 ± 6.6 | 0.709 | 48.5 ± 6.8 | 48.3 ± 7.3 | 0.918 | 48.9 ± 7.2 | 47.7 ± 6.6 | 0.361 | 48.3 ± 7.4 | 48.5 ± 6.7 | 0.868 | 48.0 ± 7.3 | 48.6 ± 6.9 | 0.643 |
| Perifoveal capillary density (%) | 42.3 ± 7.3 | 42.2 ± 5.0 | 0.913 | 42.6 ± 7.0 | 41.9 ± 5.5 | 0.609 | 42.6 ± 7.2 | 41.8 ± 5.0 | 0.496 | 42.0 ± 5.6 | 42.5 ± 6.8 | 0.720 | 41.5 ± 6.6 | 42.7 ± 6.2 | 0.388 |
| FAZ (mm ²) | 0.3 ± 0.1 | 0.4 ± 0.4 | 0.205 | 0.3 ± 0.2 | 0.4 ± 0.4 | 0.222 | 0.3 ± 0.1 | 0.4 ± 0.4 | 0.577 | 0.4 ± 0.4 | 0.3 ± 0.2 | 0.295 | 0.4 ± 0.4 | 0.3 ± 0.2 | 0.110 |
| Parafoveal RNFL thickness (μm) | 97.2 ± 18.8 | 97.2 ± 14.2 | 0.991 | 98.3 ± 18.7 | 96.0 ± 14.3 | 0.462 | 97.3 ± 17.0 | 97.0 ± 16.7 | 0.934 | 94.9 ± 16.9 | 99.0 ± 16.6 | 0.192 | 92.8 ± 19.1 | 99.6 ± 15.0 | 0.055 |
| Perifoveal RNFL thickness (μm) | 95.7 ± 11.3 | 94.2 ± 9.3 | 0.427 | 95.5 ± 11.2 | 94.4 ± 9.5 | 0.586 | 95.7 ± 10.4 | 93.9 ± 10.5 | 0.393 | 93.4 ± 12.6 | 96.3 ± 8.2 | 0.158 | 94.5 ± 11.7 | 95.3 ± 9.7 | 0.694 |
| RPC density (%) | 48.4 ± 4.8 | 46.1 ± 5.2 | 0.017 | 47.6 ± 4.6 | 47.1 ± 5.6 | 0.623 | 48.5 ± 4.2 | 45.4 ± 5.9 | 0.001 | 45.8 ± 5.9 | 48.5 ± 4.1 | 0.004 | 47.2 ± 5.7 | 47.4 ± 4.8 | 0.812 |
| Inside disc capillary density (%) | 49.3 ± 4.4 | 47.6 ± 5.2 | 0.061 | 49.2 ± 5.2 | 47.6 ± 4.4 | 0.080 | 49.3 ± 4.5 | 47.1 ± 5.2 | 0.019 | 48.2 ± 4.9 | 48.7 ± 4.9 | 0.659 | 46.8 ± 5.0 | 49.4 ± 4.6 | 0.007 |
| Peripapillary RNFL thickness (μm) | 107.3 ± 10.5 | 105.9 ± 11.2 | 0.487 | 107.1 ± 10.6 | 106.1 ± 11.1 | 0.641 | 108.9 ± 7.8 | 103.0 ± 13.7 | 0.004 | 104.3 ± 12.3 | 108.5 ± 9.1 | 0.040 | 107.4 ± 11.3 | 106.2 ± 10.6 | 0.579 |

OCT, optical coherence tomography; OCTA, optical coherence tomography angiography; CSVD, cerebral small vessel disease; DWMLs, deep white matter lesions; PWMLs, paraventricular white matter lesions; PVS, perivascular spaces; CMB, cerebral microbleed; SD, standard deviation; SRCP, superficial retinal capillary plexuses; DRCP, deep retinal capillary plexuses; FAZ, foveal avascular zone; RNFL, retinal nerve fiber layer; RPC, radial peripapillary capillary.



Statistical Analysis

Data were collected and analyzed by SPSS version 20.0 for Windows (IBM Co., Armonk, NY, USA). Continuous variables were presented as means \pm standard deviations, and categorical variables were presented as frequencies and percentages. Univariate and multivariate logistic analyses were performed to explore the relationship between OCTA parameters and CSVD. On univariate analysis, Student's *t*-test and χ^2 test were used for continuous and categorical variables, respectively. Non-normal distributions were analyzed using the Mann-Whitney *U*-test and presented as medians (interquartile ranges, IQRs). Variables exhibiting significant differences ($p < 0.05$) in the univariate analysis were included in the multivariate logistic model. All *p*-values were two-tailed, and a $p < 0.05$ was defined as statistically significant.

RESULTS

A total of 132 patients diagnosed with CSVD were screened at our center. Seventeen patients were excluded due to poor OCTA imaging quality. Finally, 115 patients (male: 40%, right eye: 50%) were enrolled and analyzed. The mean age was 65.11 ± 11.23 years. The leading comorbidity was hypertension (59.1%), whereas type 2 diabetes mellitus was the least prevalent (28.7%) (Table 1). The mean RPC network density was $47.34 \pm 5.09\%$, inside disc capillary density was $48.47 \pm 4.88\%$, parafoveal capillary density was $44.37 \pm 6.92\%$, perifoveal capillary density was $45.29 \pm 4.61\%$, and FAZ was $0.34 \pm 0.28 \text{ mm}^2$.

Univariate analysis revealed significant correlation between the severity of DWMLs and hypertension ($p = 0.014$), older age ($p < 0.001$), and lower RPC network density ($p = 0.017$) (Table 2). Multivariate logistic regression analysis showed that RPC network density (OR: 0.909; 95% CI: 0.828–0.998; $p = 0.046$)

was negatively correlated with the severity of DWMLs (Figure 1). The severity of PWMLs was correlated with hypertension ($p < 0.001$), hyperlipidemia ($p = 0.031$), older age ($p < 0.001$), and lower inside disc capillary density ($p = 0.080$) in univariate analysis. However, no independently correlated variable was found (Table 3).

Patients with lacunes were more likely to be associated with hypertension ($p = 0.004$), lower parafoveal capillary density ($p < 0.001$) and lower perifoveal capillary density ($p = 0.015$) of the SRCP, lower RPC network density ($p = 0.004$) and thinner RNFL ($p = 0.04$) compared to those without lacunes. Multivariate logistic analysis revealed that lower parafoveal capillary density of SRCP (OR: 0.889; 95% CI: 0.817–0.967; $p = 0.006$) and hypertension (OR: 3.156; 95% CI: 1.348–7.392; $p = 0.008$) were independently correlated with lacunes.

Patients in the moderate to severe PVS group had significantly higher blood pressure ($p = 0.012$), older age ($p < 0.001$), lower RPC network density ($p = 0.001$), thinner peripapillary RNFL ($p = 0.004$), and lower inside disc capillary density ($p = 0.019$). After multivariate logistic analysis, RPC network density showed a negative correlation with PVS severity (OR: 0.881; 95% CI: 0.779–0.995; $p = 0.041$).

There were significant differences between CMB patients and non-CMB patients regarding hypertension ($p = 0.024$), hyperlipidemia ($p = 0.033$), age ($p = 0.037$), and inside disc capillary density ($p = 0.007$) in the univariate analysis. However, no variables were significantly different after multivariate logistic regression analysis.

DISCUSSION

Recently, CSVD has garnered increasing attention, and there has been great demand for a simpler screening method for CSVD

in clinical practice. Anatomical, embryologic, and physiological characteristics of retinal blood vessels are similar to those of cerebral small vessels (8–10). The retina is regarded as a direct extension of the diencephalon and shares similar angiogenesis patterns. Meanwhile, vessels in the cerebral cortex (50–200 μm) and those of the retina (50–170 μm) have similar diameters and are approximately equal in size. Physiologically, the retina has a highly isolated and protected vascular system similar to that of the brain (18, 19). In 1986, Hinton et al. (20) described how neuro-degenerative changes affected the retina, lending credence to the correlation between the retina and the brain. Moreover, the fundus is the only part of the body that enables direct observation of nerves and blood vessels, thereby providing a direct path reflecting the nerves and blood vessels of the brain.

OCTA, a non-invasive imaging technique that provides high-resolution volumetric data, has been widely used in clinical practice. However, OCTA has not been applied to evaluate the correlation between fundus vessels and CSVD. In 2018, Lahme et al. analyzed 74 patients with AD and demonstrated that the Fazekas score was significantly correlated with retinal flow density rather than the area of the FAZ. However, RNFL thickness was not included in their study (21). Further, den Haan et al. (14) enrolled patients with AD and found that vessel density in the outer ring of the macula was inversely associated with the Fazekas score, whereas no correlation was identified between the RNFL thickness or FAZ and the Fazekas score. Together, these studies focused on patients with AD or mild cognitive impairment, and the sample size was small. To date, the application of OCTA in the evaluation of CSVD is lacking. We conducted this study to explore the correlation between CSVD and fundus changes revealed by OCTA.

Patients with lower RPC density had a higher Fazekas score in DWMLs rather than in PWMLs. There are some possible explanations: (1) as indicated by histological findings, PWMLs are non-ischemic. However, microcystic infarcts and patchy rarefaction of myelin which are ischemic, are associated with DWMLs (22–24); (2) anatomically, the paraventricular white matter area might be more hemodynamically determined, because this area is supplied by non-collateralizing ventriculofugal vessels arising from the subependymal arteries originating from the choroidal arteries, or from the terminal branches of the ramistriate and ventriculofugal vessels that run toward the penetrating centripetal vessels coming from the pial surface supply. Hence, the blood supply is not solely from small cerebral vessels in the periventricular white matter areas (24, 25). Conversely, deep white matter is supplied by medullary arteries arising from the cortical branches of middle cerebral arteries and has a single blood supply system, thus being more susceptible to ischemia (26).

Our study revealed a close inverse correlation between the RPC density and the Fazekas score in DWMLs. However, no correlation was detected between the Fazekas score and capillary density of the inside disc or macula. We propose a possible reason is that there are two distinct circulatory systems within the disc, the central retinal artery (CRA) and the ciliary arteries, whereas the radial peripapillary of the disc is only supplied principally by recurrent retinal arterioles arising from branches of the CRA. As

TABLE 3 | Multivariate analysis of the related factors for each type of CSVD.

| Variables | OR | 95% CI | P |
|-----------------------------------|-------|-------------|-------|
| DWMLs | | | |
| Age | 1.082 | 1.027–1.140 | 0.003 |
| Hypertension | 1.629 | 0.671–3.957 | 0.281 |
| RPC density | 0.909 | 0.828–0.998 | 0.046 |
| Inside disc capillary density | 0.966 | 0.880–1.059 | 0.459 |
| PWMLs | | | |
| Hypertensions | 3.019 | 1.196–7.626 | 0.019 |
| Age | 1.078 | 1.022–1.136 | 0.005 |
| DM | 1.498 | 0.556–4.031 | 0.424 |
| Hyperlipidemia | 1.753 | 0.693–4.432 | 0.236 |
| Inside disc capillary density | 0.999 | 0.914–1.091 | 0.975 |
| PVS | | | |
| Hypertension | 1.354 | 0.526–3.485 | 0.530 |
| Age | 1.078 | 1.020–1.138 | 0.007 |
| RPC density | 0.881 | 0.779–0.995 | 0.041 |
| Inside disc capillary density | 0.928 | 0.836–1.032 | 0.167 |
| Peripapillary RNFL thickness | 0.964 | 0.907–1.023 | 0.225 |
| Lacunae | | | |
| Hypertension | 3.156 | 1.348–7.392 | 0.008 |
| SRCP-parafoveal capillary density | 0.889 | 0.817–0.967 | 0.006 |
| SRCP-perifoveal capillary density | 1.012 | 0.892–1.147 | 0.856 |
| RPC density | 0.930 | 0.831–1.041 | 0.209 |
| Peripapillary RNFL thickness | 0.987 | 0.931–1.048 | 0.672 |
| CMB | | | |
| Age | 1.037 | 0.990–1.086 | 0.128 |
| Hypertension | 1.231 | 0.479–3.167 | 0.666 |
| DM | 1.633 | 0.572–4.661 | 0.359 |
| Hyperlipidemia | 1.75 | 0.672–4.559 | 0.252 |
| Parafoveal RNFL thickness | 0.984 | 0.959–1.009 | 0.203 |
| Inside disc capillary density | 0.924 | 0.837–1.020 | 0.117 |

CSVD, cerebral small vessel disease; OR, odds ratio; CI, confidence interval; DWMLs, deep white matter lesions; PWMLs, paraventricular white matter lesions; DM, diabetes mellitus; PVS, perivascular spaces; RPC, radial peripapillary capillary; SRCP, superficial retinal capillary plexuses; CMB, cerebral microbleed; RNFL, retinal nerve fiber layer.

a result, the radial peripapillary of the disc is more susceptible to ischemia.

In Lahme's study, the correlation between the vessel density of the RPC and the Fazekas score of WMLs was also demonstrated, which is in agreement with the findings in our study (21). However, they also reported that the vessel density of the parafoveal was related to the Fazekas score, which differed from our results. This is possibly because their study focused on patients with AD; the sample size could have also contributed to differences in the results obtained.

The present study also revealed that the lower density of RPCs was not only related to DWMLs, but the severity of PVS. Doubal et al. (27) reported that enlargement of the PVS was associated with WMLs. The PVS serves as an important conduit for the drainage of interstitial fluid to the ventricles, and it could be affected by abnormalities of the blood-brain barrier (28). Therefore, the parallel formation mechanism between

WMLs and PVS may lead to similar changes in the fundus and comparable trends in RPC density, which could explain our results (29).

Lacunae are caused by small vessel disease, and pathological vascular changes in lacunae were mainly lipid hyaline degeneration or micro atherosclerotic plaque (30). As reported previously, our study also indicated patients with lacunae exhibited lower vessel density of the parafoveal SRCP (14, 21). However, the underlying mechanism requires further exploration. We suspected that the possible reason might be that the vascular density of the parafovea was lower than that of the perifovea in healthy individuals; therefore, the parafovea may be more vulnerable to ischemia.

No independent relationship was established between deep vascular density or the thickness of the fibrous layer and lacunae. Within the retina, there were two distinct circulatory systems, the superficial retina was supplied by the CRA, and the deep retina was supplied by ciliary arteries. Unlike the ciliary arteries, the CRA is a terminal vessel. Animal studies have demonstrated that ciliary arteries transport a greater volume of blood than the retinal the blood flow (31, 32). Therefore, the deep retina with its greater blood supply was less affected by ischemia than the superficial, which may account for the lack of significant correlation between the deep vascular densities and lacunae. Further, no significant correlation was found between the thickness of the fibrous layer and lacunae, possibly because the fibrous layer is not affected in the early stage of the disease.

There were no significant differences in the parameters of the fundus between patients with and without CMB in this study. The mechanism of CMB is primarily amyloid deformation rather than ischemia, which could explain the results.

There are limitations in this study. First, this is a non-randomized study and a control group was not included. Second, although the sample size is relatively large, studies with even larger cohorts are required to confirm our conclusions. Nevertheless, our study provides practical and useful information regarding the application of OCTA in CSVD screening.

CONCLUSION

This study investigated the correlation between four types of cerebrovascular diseases and fundus changes revealed by OCTA

in a relatively large cohort. To the best of our knowledge, this is the first study to simultaneously assess four types of CSVD and to analyze PWMLs and DWMLs in parallel. The correlation between fundus parameters and CSVD suggests that OCTA is a feasible screening method for CSVD. Further studies using OCTA for CSVD screening are required to confirm our findings. OCTA parameters correlated with CSVD, with the most important being the RPC network density, which was negatively correlated with the severity of DWMLs and PVS, indicating that OCTA is a promising potential method for CSVD screening.

DATA AVAILABILITY STATEMENT

The raw data supporting the conclusions of this article will be made available by the authors, without undue reservation.

ETHICS STATEMENT

This study was approved by the Ethics Committee of Shanghai Tenth People's Hospital (No. 21k253). The patients/participants provided their written informed consent to participate in this study. Written informed consent was obtained from the individual(s) for the publication of any potentially identifiable images or data included in this article.

AUTHOR CONTRIBUTIONS

WF, XZ, PG, and JW: conception and design. WF, XZ, MW, PL, PG, and JW: analysis and interpretation. WF, XZ, MW, PL, and JH: data collection. WF, XZ, and PG: writing the manuscript. WF, XZ, MW, PL, JH, PG, and JW: final approval of the article and overall responsibility. WF, XZ, PL, JH, PG, and JW: statistical analysis. JW: obtained funding. All authors contributed to the article and approved the submitted version.

FUNDING

This work was supported by Shanghai Municipal Key Clinical Specialty (shslczdzk06102), Shanghai Science and Technology Commission (19401972804), and Start-up Fund of Shanghai Tenth People's Hospital (04.03.16.002).

REFERENCES

1. Wardlaw JM, Smith C, Dichgans M. Mechanisms of sporadic cerebral small vessel disease: insights from neuroimaging. *Lancet Neurol.* (2013) 12:483–97. doi: 10.1016/S1474-4422(13)70060-7
2. Wardlaw JM, Smith C, Dichgans M. Small vessel disease: mechanisms and clinical implications. *Lancet Neurol.* (2019) 18:684–96. doi: 10.1016/S1474-4422(19)30079-1
3. Shu J, Neugebauer H, Li F, Lulé D, Müller HP, Zhang J, et al. Clinical and neuroimaging disparity between Chinese and German patients with cerebral small vessel disease: a comparative study. *Sci Rep.* (2019) 9:20015. doi: 10.1038/s41598-019-55899-w
4. Li Q, Yang Y, Reis C, Tao T, Li W, Li X, et al. Cerebral small vessel disease. *Cell Transplant.* (2018) 27:1711–22. doi: 10.1177/0963689718795148
5. Wardlaw JM, Smith EE, Biessels GJ, Cordonnier C, Fazekas F, Frayne R, et al. Neuroimaging standards for research into small vessel disease and its contribution to ageing and neurodegeneration. *Lancet Neurol.* (2013) 12:822–38. doi: 10.1016/S1474-4422(13)70124-8
6. van Veluw SJ, Shih AY, Smith EE, Chen C, Schneider JA, Wardlaw JM, et al. Detection, risk factors, and functional consequences of cerebral microinfarcts. *Lancet Neurol.* (2017) 16:730–40. doi: 10.1016/S1474-4422(17)30196-5
7. Newman EA. Functional hyperemia and mechanisms of neurovascular coupling in the retinal vasculature. *J Cereb Blood Flow Metab.* (2013) 33:1685–95. doi: 10.1038/jcbfm.2013.145
8. Lee JY, Kim JP, Jang H, Kim J, Kang SH, Kim JS, et al. Optical coherence tomography angiography as a potential screening tool for cerebral small vessel diseases. *Alzheimers Res Ther.* (2020) 12:73. doi: 10.1186/s13195-020-00638-x

9. Baker ML, Hand PJ, Wang JJ, Wong TY. Retinal signs and stroke: revisiting the link between the eye and brain. *Stroke*. (2008) 39:1371–9. doi: 10.1161/STROKEAHA.107.496091
10. Cheung N, Mosley T, Islam A, Kawasaki R, Sharrett AR, Klein R, et al. Retinal microvascular abnormalities and subclinical magnetic resonance imaging brain infarct: a prospective study. *Brain*. (2010) 133(Pt 7):1987–93. doi: 10.1093/brain/awq127
11. Jia Y, Bailey ST, Wilson DJ, Tan O, Klein ML, Flaxel CJ, et al. Quantitative optical coherence tomography angiography of choroidal neovascularization in age-related macular degeneration. *Ophthalmology*. (2014) 121:1435–44. doi: 10.1016/j.ophtha.2014.01.034
12. Spaide RF, Klanclnik JM Jr, Cooney MJ. Retinal vascular layers imaged by fluorescein angiography and optical coherence tomography angiography. *JAMA Ophthalmol*. (2015) 133:45–50. doi: 10.1001/jamaophthol.2014.3616
13. Fazekas F, Chawluk JB, Alavi A, Hurtig HI, Zimmerman RA. MR signal abnormalities at 1.5 T in Alzheimer's dementia and normal aging. *AJR Am J Roentgenol*. (1987) 149:351–6. doi: 10.2214/ajr.149.2.351
14. den Haan J, van de Kreeke JA, van Berckel BN, Barkhof F, Teunissen CE, Scheltens P, et al. Is retinal vasculature a biomarker in amyloid proven Alzheimer's disease? *Alzheimers Dement (Amst)*. (2019) 11:383–91. doi: 10.1016/j.dadm.2019.03.006
15. Potter GM, Chappell FM, Morris Z, Wardlaw JM. Cerebral perivascular spaces visible on magnetic resonance imaging: development of a qualitative rating scale and its observer reliability. *Cerebrovasc Dis*. (2015) 39:224–31. doi: 10.1159/000375153
16. Wilson D, Ambler G, Lee KJ, Lim JS, Shiozawa M, Koga M, et al. Cerebral microbleeds and stroke risk after ischaemic stroke or transient ischaemic attack: a pooled analysis of individual patient data from cohort studies. *Lancet Neurol*. (2019) 18:653–65. doi: 10.1016/S1474-4422(19)30197-8
17. Wu J, Zhang X, Azhati G, Li T, Xu G, Liu F. Retinal microvascular attenuation in mental cognitive impairment and Alzheimer's disease by optical coherence tomography angiography. *Acta Ophthalmol*. (2020) 98:e781–e7. doi: 10.1111/aos.14381
18. Patton N, Aslam T, MacGillivray T, Pattie A, Deary IJ, Dhillon B. Retinal vascular image analysis as a potential screening tool for cerebrovascular disease: a rationale based on homology between cerebral and retinal microvasculatures. *J Anat*. (2005) 206:319–48. doi: 10.1111/j.1469-7580.2005.00395.x
19. London A, Benhar I, Schwartz M. The retina as a window to the brain—from eye research to CNS disorders. *Nat Rev Neurol*. (2013) 9:44–53. doi: 10.1038/nrneurol.2012.227
20. Hinton DR, Sadun AA, Blanks JC, Miller CA. Optic-nerve degeneration in Alzheimer's disease. *New Engl J Med*. (1986) 315:485–7. doi: 10.1056/NEJM198608213150804
21. Lahme L, Esser EL, Mihailovic N, Schubert F, Laueremann J, Johnen A, et al. Evaluation of ocular perfusion in Alzheimer's disease using optical coherence tomography angiography. *J Alzheimers Dis*. (2018) 66:1745–52. doi: 10.3233/JAD-180738
22. Fazekas F, Schmidt R, Scheltens P. Pathophysiological mechanisms in the development of age-related white matter changes of the brain. *Dement Geriatr Cogn Disord*. (1998) 9(Suppl. 1):2–5. doi: 10.1159/000051182
23. Thomas AJ, O'Brien JT, Barber R, McMeekin W, Perry R. A neuropathological study of periventricular white matter hyperintensities in major depression. *J Affect Disord*. (2003) 76:49–54. doi: 10.1016/S0165-0327(02)00064-2
24. van Swieten JC, van den Hout JH, van Ketel BA, Hijdra A, Wokke JH, van Gijn J. Periventricular lesions in the white matter on magnetic resonance imaging in the elderly. A morphometric correlation with arteriosclerosis and dilated perivascular spaces. *Brain*. (1991) 114(Pt 2):761–74. doi: 10.1093/brain/114.2.761
25. Rowbotham GF, Little E. A new concept of the circulation and the circulations of the brain. The discovery of the surface arteriovenous shunts. *Br J Surg*. (1965) 52:539–42. doi: 10.1002/bjs.1800520714
26. Read SJ, Pettigrew L, Schimmel L, Levi CR, Bladin CF, Chambers BR, et al. White matter medullary infarcts: acute subcortical infarction in the centrum ovale. *Cerebrovasc Dis*. (1998) 8:289–95. doi: 10.1159/000015868
27. Doubal FN, MacLulich AM, Ferguson KJ, Dennis MS, Wardlaw JM. Enlarged perivascular spaces on MRI are a feature of cerebral small vessel disease. *Stroke*. (2010) 41:450–4. doi: 10.1161/STROKEAHA.109.564914
28. Wardlaw JM, Doubal F, Armitage P, Chappell F, Carpenter T, Muñoz Maniega S, et al. Lacunar stroke is associated with diffuse blood-brain barrier dysfunction. *Ann Neurol*. (2009) 65:194–202. doi: 10.1002/ana.21549
29. Pantoni L, Garcia JH. Pathogenesis of leukoaraiosis: a review. *Stroke*. (1997) 28:652–9. doi: 10.1161/01.STR.28.3.652
30. Fisher CM. Lacunes: small, deep cerebral infarcts. *Neurology*. (1965) 15:774–84. doi: 10.1212/WNL.15.8.774
31. Alm A, Bill A. Ocular and optic nerve blood flow at normal and increased intraocular pressures in monkeys (*Macaca irus*): a study with radioactively labelled microspheres including flow determinations in brain and some other tissues. *Exp Eye Res*. (1973) 15:15–29. doi: 10.1016/0014-4835(73)90185-1
32. Wang L, Fortune B, Cull G, McElwain KM, Cioffi GA. Microspheres method for ocular blood flow measurement in rats: size and dose optimization. *Exp Eye Res*. (2007) 84:108–17. doi: 10.1016/j.exer.2006.09.005

Conflict of Interest: The authors declare that the research was conducted in the absence of any commercial or financial relationships that could be construed as a potential conflict of interest.

Publisher's Note: All claims expressed in this article are solely those of the authors and do not necessarily represent those of their affiliated organizations, or those of the publisher, the editors and the reviewers. Any product that may be evaluated in this article, or claim that may be made by its manufacturer, is not guaranteed or endorsed by the publisher.

Copyright © 2022 Fu, Zhou, Wang, Li, Hou, Gao and Wang. This is an open-access article distributed under the terms of the Creative Commons Attribution License (CC BY). The use, distribution or reproduction in other forums is permitted, provided the original author(s) and the copyright owner(s) are credited and that the original publication in this journal is cited, in accordance with accepted academic practice. No use, distribution or reproduction is permitted which does not comply with these terms.